QoE-Guaranteed and Power-Efficient Network Operation for Cloud Radio Access Network With Power Over Fiber

Katsuya Suto, *Student Member, IEEE*, Keisuke Miyanabe, *Student Member, IEEE*, Hiroki Nishiyama, *Senior Member, IEEE*, Nei Kato, *Fellow, IEEE*, Hirotaka Ujikawa, *Member, IEEE*, and Ken-Ichi Suzuki, *Member, IEEE*

***Abstract*—A concept of cloud radio access networks (C-RANs) is becoming a popular solution to support the required communication quality for new emerging service in the future network environment, i.e., more than 10 Gbps capacity, less than 1 ms latency, and connectivity for numerous devices. In this paper, we envision a C-RAN based on passive optical network (PON) exploiting power over fiber (PoF), which achieves low installation and operation costs since it is capable of providing communication services without external power supply for large amount of remote radio heads (RRHs). This network, however, needs to reduce the optical transmission power of PoF due to the fiber fuse issue. Additionally, the diversification of services, devices, and personality indicates the need to improve user satisfaction, i.e., quality of experience (QoE), based on the user's perspective, which is different from previous approaches that aim to guarantee quality of services (QoS). Therefore, we propose a QoE-guaranteed and power-efficient network operation strategy. Our proposed operation is able to reduce the transmission power while satisfying the QoE constraint by controlling both the schedule of RRH's sleep and optical transmission power of PoF. Furthermore, the effectiveness of our proposed operation scheme is evaluated through extensive computer simulations.**

***Index Terms*—Cloud radio access network (C-RAN), QoE-guaranteed and power-efficient network operation, quality of experience (QoE), sleep scheduling.**

I. Introduction

FUTURE mobile networks are required to support new emerging services with a high network capacity, as well as reduce communication latency and provide connectivity for numerous devices, e.g., three-dimensional (3-D) video streaming/meeting, augmented reality (AR), online big data mining, real-time Internet of Things (IoT), and so forth [1]–[3]. A network architecture utilizing super-dense small cell deployments and centralized resource management, i.e., cloud radio access networks (C-RANs), have attracted much attention as a cornerstone to achieve the aforementioned requirements [4], [5]. In this architecture, small cells are capable of providing high communication capacity between remote radio head (RRH) and users, and a central office (CO) connects with RRHs via high-speed fronthaul links and combines the managements of users and RRHs in order to fulfill the required capacity and latency [6], [7].

Although C-RAN is expected as a promising future mobile architecture, it needs higher installation and operation costs due to the following reasons: 1) since the amount of traffic between the CO and RRHs is much higher in contrast with the traditional RAN, high-speed links are required. However, setting up private optical-fiber cables to each RRH indicates a high installation cost and 2) provision of external power supply to all RRHs will involve high cost, especially in the case of deployment in places lacking external power supply. To this end, passive optical network (PON) exploiting power over fiber (PoF) is recognized as the key enabling technology [8]–[10]. In PON with PoF, an optical splitter is used to enable a single optical-fiber cable to serve multiple RRHs, and an optical line terminal (OLT) that aggregates multiple RRHs supplies power to RRHs through the optical-fiber cable.

However, we need to reduce the transmission power of OLT for our envisioned network since supplying power above a certain level may cause the fiber fuse effect. To cope with this issue, the recent investigations on PoF are trying to develop fiber cables that are able to transmit optical signal with few watts and to create RRHs that are operated with low power consumption. In contrast to these works, this paper focuses on the investigation of the power-efficient network operation in order to tackle this issue. This approach is absolutely imperative since the improvement of physical performance has limitations.

On the other hand, the emergence of various kinds of services indicates the need to improve the overall performance from a user's perspective [11]. Indeed, network operators and service providers are now switching their focus from network quality of service (QoS) to user quality of experience (QoE). According to many investigations accomplished by [12]–[14], the QoE value has a slightly different method of measurement from QoS value since QoE is determined by user context such as age, gender, region, personality, and so forth [15], [16]. Consequently, it can be said that a QoE-guaranteed network operation is essential for our envisioned C-RAN [17], [18].

Manuscript received June 22, 2015; revised January 04, 2016; accepted January 04, 2016. Date of publication February 11, 2016; date of current version February 25, 2016.

K. Suto, K. Miyanabe, H. Nishiyama, and N. Kato are with the Graduate School of Information Sciences (GSIS), Tohoku University, Sendai 980 8579, Japan (e-mail: katsuya.suto@it.is.tohoku.ac.jp; keisuke.miyanabe@it.is.tohoku.ac.jp; bigtree@it.is.tohoku.ac.jp; kato@it.is.tohoku.ac.jp).

H. Ujikawa and K.-I. Suzuki are with the Access Network Service Systems Laboratories, NTT Corporation, Yokosuka 239 0847, Japan (e-mail: ujikawa.hirotaka@lab.ntt.co.jp; suzuki.kenichi@lab.ntt.co.jp).

Digital Object Identifier 10.1109/TCSS.2016.2518208

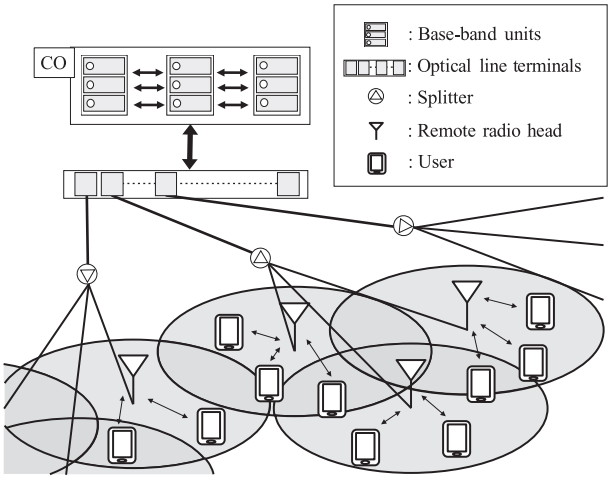

Fig. 1. Architecture of our envisioned C-RAN based on PON exploiting PoF.

In this paper, we aim to demonstrate the QoE-guaranteed and power-efficient network operation. First, we describe the mathematical model of our envisioned C-RAN such as an energy harvesting model and a battery-powered model of RRHs. Then, we show a correlation model between the communication distance from RRH to user and QoE value, which is used for our proposed network operation. Furthermore, we present a joint control method of RRH sleep and transmission power of OLTs to reduce the transmission power while guaranteeing the individual QoE of users.

This paper is organized as follows. Section II describes the system model of our considered C-RAN architecture. The correlation between the QoE value and transmission distance is elucidated in Section III. Our proposed QoE-guaranteed and power-efficient network operation scheme is explained in Section IV. We present the performance evaluation in Section V. Finally, this paper is concluded in Section VI.

II. Envisioned C-RAN With PoF

In this section, we introduce our envisioned C-RAN architecture and the roles of each network component. Furthermore, we describe the system model of our envisioned C-RAN.

A. Overview

Our envisioned C-RAN is based on PON exploiting the PoF technology as shown in Fig. 1. As shown in this figure, our assumed network can be divided into three components, i.e., the CO, the OLTs, and the RRHs. In the remainder of this section, the roles of CO, OLT, and RRH are described.

Traditional RAN architecture utilizes the distributed resource management. In this architecture, a base-band unit (BBU), which is a function to manage the resource and interference, is put on each base station. In contrast to this architecture, C-RAN deploys BBUs in a CO in order to control numerous RRHs via an "intelligent brain." This architecture can effectively manage the complex functions of numerous RRHs, e.g., multiple input multiple output (MIMO), coordinated multipoint (CoMP), and handover. In addition to wireless components, the CO controls the optical components in C-RAN. This means that the CO decides the optical resource allocation and transmission power of OLTs.

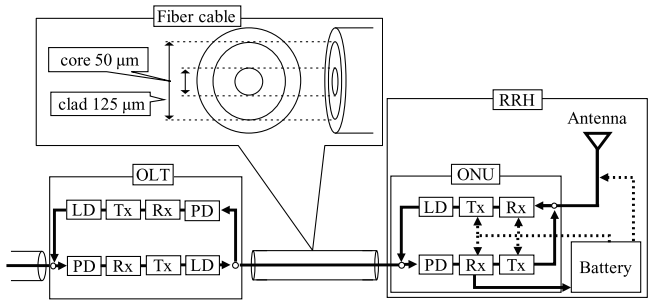

Fig. 2. PoF in our considered network.

Our envisioned C-RAN utilizes the PON to construct a fronthaul network between OLTs and RRHs. Each OLT in our envisioned network has two roles for the connected RRHs as follows: 1) data communication between the OLT and RRHs and 2) power supply to RRHs. For data transmission to multiple RRHs, we assume that wavelength division multiplexing (WDM) is used for resource allocation. On the other hand, we assume that RRHs transmit data to the OLT based on time division multiplexing (TDM). For power supply to RRHs, we assume the usage of PoF technology which is able to convert optical signal to electrical power. Since PON has a feature of broadcast from OLT to RRHs [19] and some RRHs receive data which are not meant for them, the "unnecessary data" is converted to electric power by PoF technology and used to power its own operation. The OLT is, therefore, used by the CO to supply electric power to the RRHs by using the unnecessary data.

In the envisioned network, it is considered that numerous RRHs are deployed. As shown in Fig. 2, each RRH is composed of three modules, i.e., the optical network unit (ONU) module, battery module, and antenna module. Furthermore, Fig. 2 illustrates how the ONU module of an RRH communicates with the OLT. The optical fiber used for communication between the OLT and the ONU module of the RRH is assumed to be a multimode fiber having core diameter of 50 μm and clad diameter of 125 μm [20]. In case of downlink communication, the OLT receives data from the CO at its Rx component [21]. The received data are converted into optical signal at laser diode (LD), which is transmitted over the fiber to the ONU of RRHs. The RRH, which receives necessary data, converts the optical signal into electric signal, which is transmitted to users via antenna module. In case of receiving unnecessary data, the optical signal is converted into electrical power, which is stored in battery module via Rx component. Here, the OLT informs the accommodated RRHs of the address of transmission data by sending the signal including the address information in advance. The battery module continuously stores the converted power and supplies the stored electricity to ONU and antenna modules for their operation. Our supposed RRHs also have a sleep function, which reduces power consumption of RRHs by turning down some modules. However, the PD and Rx components used to receive the transmitted signal from OLT, and the battery module cannot enter in sleep state all times since they are required to harvest electric power [22].

B. System Model

Our supposed C-RAN consists of a single CO, $|L|$ OLTs, and $|R|$ RRHs, where the set of OLTs and that of RRHs are defined as $L = \{l_1, l_2, \ldots, l_{|L|}\}$ and $R = \{r_1, r_2, \ldots, r_{|R|}\}$, respectively. Since each OLT connects to multiple RRHs via PON, we define $R_{l_k} = \{r_{l_k,1}, r_{l_k,2}, \ldots, r_{l_k,|R_{l_k}|}\}$, which denotes the set of RRHs that connect to the OLT l_k. Here, note that the number of branches of the splitter in PON θ is decided as $|R_{l_k}|$. Additionally, the distance of the link from OLT l_k to RRH $r_{l_k,i}$ is defined as $d^{l_k}_{r_{l_k,i}}$. In the PON with PoF, the optical transmission signals from OLTs are attenuated because of the fiber attenuation, the power branch at the splitter, and the loss of photoelectric conversion. Supposed that O_{l_k}, $\varphi(d^{l_k}_{r_{l_k,i}})$, and ρ are the transmission power of OLT l_k, power loss factor due to transmission distance, and conversion efficiency, respectively, the received power of RRH $r_{l_k,i}$ $O_{r_{l_k,i}}$ can be expressed as

$$O_{r_{l_k,i}} = \frac{\rho\varphi(d^{l_k}_{r_{l_k,i}})O_{l_k}}{\theta} \tag{1}$$

$$\varphi(d^{l_k}_{r_{l_k,i}}) = 10^{(-d^{l_k}_{r_{l_k,i}}\varphi_{\text{dB}}/10)} \tag{2}$$

where φ_{dB} is the fiber attenuation in dB/km [23]. Furthermore, since the Rx module of the RRHs converts the unnecessary transmission signal to electric power and the battery module stores the converted power, the harvested power of RRH $r_{l_k,i}$ $H_{r_{l_k,i}}$ can be expressed as

$$H_{r_{l_k,i}} = O_{r_{l_k,i}}(1-\omega_{r_{l_k,i}}) = \frac{\rho\varphi(d^{l_k}_{r_{l_k,i}})O_{l_k}}{\theta}(1-\omega_{r_{l_k,i}}) \tag{3}$$

where $\omega_{r_{l_k,i}}$ is the ratio of signal addressed to RRH $r_{l_k,i}$.

Let $U_{r_{l_k,i}} = \{u_1^{r_{l_k,i}}, u_2^{r_{l_k,i}}, \ldots, u_{|U_{r_{l_k,i}}|}^{r_{l_k,i}}\}$ be the set of users to which the RRH $r_{l_k,i}$ provides communication service, where the set of total users is defined as $U = \{u_1, u_2, \ldots, u_{|U|}\}$ and each RRH has constraints such as the maximum number of accommodated users $\overline{M}$ and maximum transmission range $\overline{C}$. Additionally, based on the set information $U_{r_{l_k,i}}$ for all $r_{l_k,i}$, we can derive the set of users that are virtually connected to the OLT l_k U_{l_k} which is expressed as

$$U_{l_k} = U_{r_{l_k,1}} \bigcup U_{r_{l_k,2}} \bigcup \cdots \bigcup U_{r_{l_k,|R_{l_k}|}}. \tag{4}$$

Since each OLT allocates the orthogonal bandwidth to the connected RRHs and the amount of bandwidth to each RRH is decided based on the number of accommodated users of the RRH, the allocated bandwidth for the RRH $r_{l_k,i}$ $B_{r_{l_k,i}}$ is calculated with the ratio of accommodated users of RRH $r_{l_k,i}$ $f_{r_{l_k,i}}$ as follows:

$$B_{r_{l_k,i}} = B_{l_k} f_{r_{l_k,i}} = B_{l_k}\frac{|U_{r_{l_k,i}}|}{|U_{l_k}|} \tag{5}$$

where B_{l_k} denotes the total bandwidth assigned to the downlink of OLT l_k in our envisioned PON.

In the envisioned C-RAN, each RRH stores the harvested energy to the battery module, and the energy is consumed in its own operation. Additionally, since the power consumption of RRHs in sleep state E_{sleep} is smaller than that in active state E_{active}, some RRHs enter in sleep state if the energy in their battery is below a certain level. Let $q_{r_{l_k,i}}$ be the resource utilization of the link between OLT l_k and the RRH $r_{l_k,i}$. While the RRH $r_{l_k,i}$ in active state receives the signal addressed to it with the ratio $w_{r_{l_k,i}} = q_{r_{l_k,i}} f_{r_{l_k,i}}$, the OLT would never transmit signal addressed to the RRH in sleep state (i.e., $w_{r_{l_k,i}} = 0$). Therefore, the harvested power in sleep state $H^{\text{sleep}}_{r_{l_k,i}}$ and that in active state $H^{\text{active}}_{r_{l_k,i}}$ can be expressed as

$$H^{\text{sleep}}_{r_{l_k,i}} = O_{r_{l_k,i}} \tag{6}$$

$$H^{\text{active}}_{r_{l_k,i}} = O_{r_{l_k,i}}(1 - q_{r_{l_k,i}} f_{r_{l_k,i}}). \tag{7}$$

Supposed that the time is divided into multiple time slots with length τ and the state of each RRH is decided at each time slot, the amount of battery of RRH $r_{l_k,i}$ in sleep state at the end of time slot t $T^{\text{sleep}}_{r_{l_k,i}}(t)$ and that in active state $T^{\text{active}}_{r_{l_k,i}}(t)$ can be expressed as

$$\begin{aligned} T^{\text{sleep}}_{r_{l_k,i}}(t) &= T_{r_{l_k,i}}(t-1) + (H^{\text{sleep}}_{r_{l_k,i}} - E_{\text{sleep}})\tau \\ T^{\text{active}}_{r_{l_k,i}}(t) &= T_{r_{l_k,i}}(t-1) + (H^{\text{active}}_{r_{l_k,i}} - E_{\text{active}})\tau \end{aligned} \tag{8}$$

where $T_{r_{l_k,i}}(t-1)$ denotes the amount of battery of RRH $r_{l_k,i}$ at previous time slot $t-1$. Additionally, since only RRHs that are able to operate during a time slot can be chosen as active RRHs, we decide whether to let the RRH $r_{l_k,i}$ enter in active state at time slot t or not, based on the following condition:

$$T_{r_{l_k,i}}(t) + (\overline{H}^{\text{active}}_{r_{l_k,i}} - E_{\text{active}})\tau > 0 \tag{9}$$

where $\overline{H}^{\text{active}}_{r_{l_k,i}}$ is the maximum harvested power of RRH $r_{l_k,i}$, which is decided based on the maximum transmission power of OLT l_k, $\overline{O}_{l_k}$.

C. RRHs Deployment

This section presents our considered strategy to distribute RRHs in the service area. In the conventional strategy, the RRHs connected to the same OLT are distributed to a nearby area due to the simplicity of resource and interference management. However, this results in higher transmission power of OLTs when the traffic (or user) concentrates in a specific area. Consequently, we introduce a scattered strategy that distributes RRHs connected to the same OLT to a distinct (or distant) area. In the envisioned network, this approach can be realized because all RRHs are virtually managed by the CO without consideration of the connected OLTs.

Fig. 3 shows an example of the scattered deployment strategy. A service area $\boldsymbol{A}$ is defined as a square which has dimensions of γ meters wide and deep. Additionally, area A is divided into $|R_l|$ subareas since we choose an RRH from each OLT l_k and distribute the chosen RRHs to the subareas. In other words, each subarea has $|L|$ RRHs that connect to the different OLTs. For simplicity, supposed that $g = \sqrt{|R_l|}$ is an integral number, each subarea $\boldsymbol{a_i}$ becomes a square which has

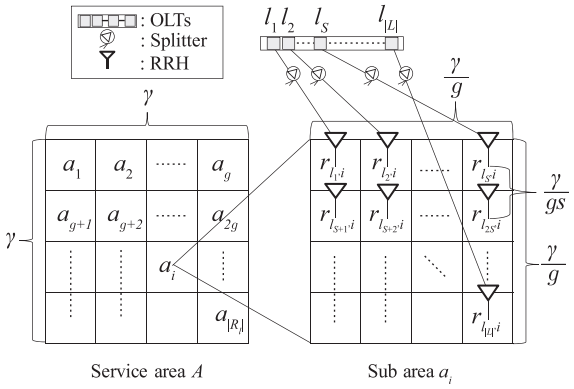

Fig. 3. Our considered RRH deployment.

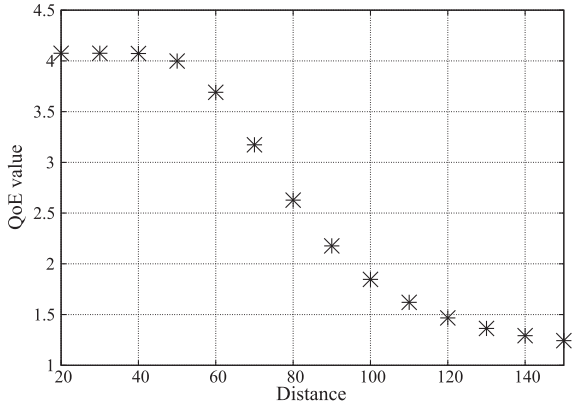

Fig. 4. Correlation between QoE value and transmission distance.

dimensions of γ/g meters wide and deep. Therefore, by using a $g \times g$ matrix, $\boldsymbol{A}$ can be expressed as

$$\boldsymbol{A} = \begin{bmatrix} \boldsymbol{a}_1 & \boldsymbol{a}_2 & \boldsymbol{a}_3 & \dots & \boldsymbol{a}_g \\ \boldsymbol{a}_{g+1} & \boldsymbol{a}_{g+2} & \boldsymbol{a}_{g+3} & \dots & \boldsymbol{a}_{2g} \\ & \vdots & & \ddots & \\ \boldsymbol{a}_{g^2-g+1} & \boldsymbol{a}_{g^2-g+2} & \boldsymbol{a}_{g^2-g+3} & \dots & \boldsymbol{a}_{|R_l|} \end{bmatrix}. \quad (10)$$

Furthermore, the subarea $\boldsymbol{a_i}$ is also divided into $|L|$ cells to which $|L|$ RRHs that are chosen from each R_{l_k} are distributed. Here, supposed that $s = \sqrt{|L|}$ is an integral number, each cell becomes a square which has dimensions of $\gamma/g/s$ meters wide and deep. In the scattered deployment, since we choose RRHs $r_{l_k,i}$ for the kth cell in subarea $\boldsymbol{a_i}$, the $s \times s$ matrix, $\boldsymbol{a_i}$, that indicates the location of RRHs, can be expressed as

$$\boldsymbol{a}_i = \begin{bmatrix} r_{l_1,i} & r_{l_2,i} & r_{l_3,i} & \dots & r_{l_s,i} \\ r_{l_{s+1},i} & r_{l_{s+2},i} & r_{l_{s+3},i} & \dots & r_{l_{2s},i} \\ & \vdots & & \ddots & \\ r_{l_{s^2-s+1},i} & r_{l_{s^2-s+2},i} & r_{l_{s^2-s+3},i} & \dots & r_{l_{|L|},i} \end{bmatrix}. \quad (11)$$

Supposed that the RRHs are distributed to the middle of each cell, the distance between neighbor RRHs, e.g., the distance between $r_{l_1,i}$ and $r_{l_2,i}$, is given as $\gamma/g/s$.

III. Correlation Between Transmission Distance and QoE Value

This section presents the impact of distance between RRH and user on the QoE value in voice over IP (VoIP) services. Some mathematical expressions and numerical results are presented to show the correlation.

While the QoE value is defined as a function of multiple influence factors including some QoS factors [24], [25], we focus on packet loss in order to derive the fundamental correlation in VoIP services. According to the investigation made in [26], the correlation between QoE value Q and packet loss probability $P(d)$ is modeled by the exponential function as

$$Q = \alpha e^{-\delta P(d)} + \beta \quad (12)$$

where α, β, and δ denote the parameters of the function that are retrieved by means of nonlinear regression. Additionally, in order to model the QoE in different network and user environments, we need to derive the appropriate values of α, β, and δ by using the observational data in the actual environment. The investigation made in [24] has conducted an experiment to measure the mean opinion scores (MOS) with different packet loss probabilities in the actual situation. According to this paper, the exponential interdependency of QoE value Q and packet loss probability $P(d)$ are given as

$$Q = 3.01e^{-4.473P(d)} + 1.065. \quad (13)$$

On the other hand, it is well known that the packet loss probability increases with higher transmission distance because of the channel fading due to the path loss [27], [28]. According to (19) described in [28], in the data transmission without retransmission control, the packet loss probability function $P(d)$ is expressed with transmission range of RRH C, distance from RRH to users d, and a positive integer value for fading parameter m as

$$P(d) = \frac{(d^2 m)^m}{\Gamma(m)} \int_0^{1/C^2} z^{m-1} e^{-d^2 m z} dz. \quad (14)$$

We redefine the original function of m described in (20) in [28] with the continuous value of d as

$$m = \lambda^{\mu/d} - \sigma. \quad (15)$$

Note that λ, μ, and σ denote the parameters that are set to model the exact communication environment.

Fig. 4 shows the QoE value with different transmission distances from RRH to user. This result is calculated based on (13)–(15) and the parameters are set as follows: $C = 150$ m, $\lambda = 1.5$, $\mu = 150$, and $\sigma = 0.5$. As shown in Fig. 4, the QoE value is approximately the same value when the transmission distance is below 50 m. From 50 m, it exponentially decreases with the increase of the transmission distance. It is obviously understood that network operators can guarantee the QoE value by connecting RRHs to the users whose distance is less than a distance threshold. In other words, the distance threshold decides the associated users for each RRH to guarantee their QoE values. For instance, in the case of Fig. 4, the distance threshold of RRHs is set to 50 m if the guaranteed QoE value is set to 4 by network operators.

Procedure 1. QoE-guaranteed and power-efficient network operation

1: Given: guaranteed QoE value, $|Q|$, transmission range, C
2: /* Decide distance threshold by analyzing the fitting function of Q in area A */
Run Distance Threshold Decision Function,
$\Psi \leftarrow$ DTDF$(|Q|, C)$
3: /* Control the sleep of RRHs and the transmission power of OLTs */
Run Sleep and Power Control Function, SPCF(Ψ)

Function 1. DTDF $(|Q|, C)$

1: Derive the parameters, α, β, and δ, in (12) based on measurement data of users
2: Decide distance threshold, Ψ, based on the fitting function of Q and guaranteed QoE value, $|Q|$
3: **return** Ψ

IV. Proposed QoE-Guaranteed and Power-Efficient Network Operation

In this section, we describe the proposed network operation scheme for our envisioned C-RAN. Our scheme aims to minimize the transmission power of each OLT while guaranteeing QoE values of individuals.

Procedure 1 shows our proposed QoE-guaranteed and power-efficient network operation. The CO executes this procedure at each time slot t. In this scheme, the guaranteed QoE value $|Q|$ and transmission range of RRHs C are previously set by the network operator. Also, this operation is classified into two functions, i.e., the distance threshold decision function (DTDF) and the sleep and power control function (SPCF). While DTDF decides the distance threshold for guaranteeing the required QoE value, SPCF jointly controls the state of RRHs, i.e., either sleep or active state, and the transmission power of OLTs based on the distance threshold.

First, the CO executes DTDF $(|Q|, C)$. Since the QoE value depends on user context, region, and time, we need to derive the adequate function of QoE in real-time based on (12). Therefore, the CO first estimates the appropriate parameters α, β, and δ by using the least-square technique [29], [30]. Here, the CO uses a large number of measurement data of users who are in the focused area and the data are observed and stored into the CO beforehand. Afterwards, the CO can construct the relationship between the QoE value and transmission distance from RRHs to users based on the transmission range C, and the derived function of QoE. By using the derived relationship and the guaranteed QoE value $|Q|$, the CO decides the distance threshold Ψ, in which the QoE value of users can be guaranteed.

Then, the CO executes SPCF(Ψ) by using the derived Ψ. First, the CO constructs a set of candidate RRHs $\dot{R}$, which will enter active state. Here, the RRHs that satisfy the aforementioned condition (9) are chosen as the candidates. On the other hand, since the other RRHs, i.e., RRHs in $R - \dot{R}$, do not have enough power for the operation until the next time slot $(t+1)$,

Function 2. SPCF(Ψ)

1: Construct a set of candidate RRHs, $\dot{R}$
2: let RRHs in $R - \dot{R}$ enter sleep state
3: **while** $\dot{R} \neq \emptyset$ and $U \neq \emptyset$ **do**
4: Choose $r'_{l_k,i}$ which has maximum amount of power
5: $\dot{R} \leftarrow \dot{R} - \{r'_{l_k,i}\}$
6: Construct a set of candidate users for $r'_{l_k,i}$, $\dot{U}_{r'_{l_k,i}}$
7: **while** $\dot{U}_{r'_{l_k,i}} \neq \emptyset$ and $|U_{r'_{l_k,i}}| < \overline{M}$ **do**
8: Choose $u_{r'_{l_k,i}}$ who has minimum distance to $r'_{l_k,i}$
9: $\dot{U}_{r'_{l_k,i}} \leftarrow \dot{U}_{r'_{l_k,i}} - \{u_{r'_{l_k,i}}\}$
10: $U_{r'_{l_k,i}} \leftarrow U_{r'_{l_k,i}} + \{u_{r'_{l_k,i}}\}$
11: **end while**
12: **if** $|U_{r'_{l_k,i}}| > 0$ **then**
13: let $r'_{l_k,i}$ enter active state
14: $U \leftarrow U - U_{r'_{l_k,i}}$
15: **else**
16: let $r'_{l_k,i}$ enter sleep state
17: **end if**
18: **end while**
19: let RRHs in $\dot{R}$ enter sleep state
20: **while** $k < |L|$ **do**
21: Decide transmission power of l_k, O_{l_k}, according to (16)
22: $k \leftarrow k + 1$
23: **end while**

the CO lets these RRHs enter sleep state. Then, it will continue to decide the state of candidate RRHs until it finishes the state decision for all candidates or user association to the RRHs for all users.

In deciding the state of RRHs, the CO first chooses the RRH $r'_{l_k,i}$, which has the maximum amount of power from the set of candidates $\dot{R}$ and then removes $r'_{l_k,i}$ from $\dot{R}$. After this, the CO constructs a set of candidate users $\dot{U}_{r'_{l_k,i}}$, in which users satisfy the distance threshold Ψ, i.e., transmission distance between users and RRH $r'_{l_k,i}$ is shorter than Ψ. Then, the CO continues to decide the users accommodated by RRH $r'_{l_k,i}$ until the set of candidates becomes empty or the number of accommodated users reaches the maximum value $\overline{M}$. In selecting the users to be accommodated, the CO chooses the user $u_{r'_{l_k,i}}$ in order of increasing distance from the closest user. Then, the CO removes $u_{r'_{l_k,i}}$ from the set of candidate users $\dot{U}_{r'_{l_k,i}}$ and adds $u_{r'_{l_k,i}}$ to the set of accommodated users $U_{r'_{l_k,i}}$. After finishing the user selection, the CO decides the state of RRH $r'_{l_k,i}$. The CO should let RRH $r'_{l_k,i}$ enter active state if RRH $r'_{l_k,i}$ accommodates at least one user, i.e., $|U_{r'_{l_k,i}}| > 0$. On the other hand, if there is no users accommodated by RRH $r'_{l_k,i}$, the CO lets RRH $r'_{l_k,i}$ enter sleep state. Then, once the CO finishes the user association process, it lets the rest of the candidate RRHs in $\dot{R}$ enter sleep state. Finally, the CO decides the transmission power of OLT l_k O_{l_k}, which is expressed with the maximum value of the required transmission power for the connected RRHs $O_{l_k}^{r_{l_k,i}}$ as follows:

$$O_{l_k} = \max_{r_{l_k,i} \in R_{l_k}} O_{l_k}^{r_{l_k,i}} \tag{16}$$

TABLE I
EVALUATION SETTINGS

Parameter	Value
Simulation time	100 s
Length of time slot	10 s
Size of service area	$450 \times 450\,\mathrm{m}^2$
Number of OLTs	9
Number of RRHs connected to each OLT	4
Power consumption of RRH in active state	1.5 W
Power consumption of RRH in sleep state	0.7 W
Amount of battery at $t = 0$	30 J
Maximum transmission power of OLT	8 W
Conversion efficiency	0.6
Fiber attenuation	0.25 db/km
Resource utilization	1 %
Transmission range of RRH	150 m
Maximum number of accommodated users	15
Fading parameter	$m = 1.5^{150/d} - 0.5$

where the value of $O_{l_k}^{r_{l_k,i}}$ in case of sleep state can be calculated with the margin of battery ε as

$$O_{l_k}^{r_{l_k,i}} = \frac{\theta}{\rho\varphi(d_{r_{l_k,i}}^{l_k})}\left(\frac{\varepsilon - T_{r_{l_k,i}}(t)}{\tau} + E_{\text{sleep}}\right) \tag{17}$$

and the value of $O_{l_k}^{r_{l_k,i}}$ in case of active state can be decided as

$$O_{l_k}^{r_{l_k,i}} = \frac{\theta}{\rho\varphi(d_{r_{l_k,i}}^{l_k})(1 - q_{r_{l_k,i}} f_{r_{l_k,i}})} \cdot \left(\frac{\varepsilon - T_{r_{l_k,i}}(t)}{\tau} + E_{\text{active}}\right). \tag{18}$$

V. PERFORMANCE EVALUATION

In this section, we confirm the effectiveness of our proposed QoE-guaranteed and power-efficient network operation in our envisioned C-RAN in comparison with the conventional scheme, by using extensive simulations. Furthermore, we evaluate the performance of the proposed scheme in different scenarios, i.e., different user densities and different margins of battery.

A. Parameter Settings

Table I describes the settings of our simulations. The simulations are executed for 100 s, which is divided into ten time slots. In these simulations, a service area is defined as a square which has dimensions of 450 m wide and deep. Users are evenly distributed into this area. As a system configuration, we consider that there exist a single CO and nine OLTs, which are located in the middle of this area. Additionally, since each OLT connects to 4 RRHs, there exist 36 RRHs. The power consumption of each RRH in active state and that in sleep state are set to 1.5 W [20] and 0.7 W [31], respectively. Additionally, we assume that each RRH stores 30 J in its battery at time slot $t = 0$. As a PoF model, the maximum transmission power of each OLT, conversion efficiency, fiber attenuation, and resource utilization of the communication from an OLT to any RRHs, are set to 8 W, 0.6, 0.25 db/km, and 1%, respectively [23], [32]. Furthermore, the transmission range of each RRH and maximum number of accommodated users are set to 150 m and 15, respectively. As a fading model, λ, μ, and σ are set to 1.5, 150, and 0.5, respectively. To model the relation between QoE value and packet loss probability, the following equation is used in the simulations:

$$Q = 4.05e^{-8.473P(d)} + 0.965. \tag{19}$$

TABLE II
RELATION BETWEEN QOE LEVEL AND DISTANCE THRESHOLD IN THE SIMULATION ENVIRONMENTS

QoE level	1	2	3	4	5
Distance threshold (m)	137	81	70	60	41

B. Performance Comparison

In order to verify the effectiveness of our proposed network operation, we compare the performance between it and the conventional scheme. While our proposed scheme changes distance threshold based on the guaranteed QoE level, the conventional scheme uses a constant distance threshold (i.e., 70 m). In this simulation, we evaluate the performance by changing the guaranteed QoE level from 1 to 5. The adequate distance threshold to guarantee the certain QoE level is listed as shown in Table II. Additionally, the total number of users and the margin of battery are set to 100 and 2 J, respectively.

Fig. 5(a) demonstrates the cumulative sum of average transmission power of OLTs in different QoE settings. The average transmission power of OLTs in the conventional scheme does not change according to QoE level and is the same as the proposed scheme in $|Q| = 3$. In contrast to this, the proposed scheme reduces the average transmission power of OLTs when the guaranteed QoE level is lower than 3. Although higher transmission power is required in the case that the guaranteed QoE level is higher than 3, the difference is small compared to the case of 1 and 2 because the transmission power increases logarithmically with the increase of QoE level. Therefore, the transmission power in the proposed scheme is lower than the conventional scheme.

Fig. 5(b) shows the cumulative sum of users satisfying the QoE levels. As shown in this figure, the proposed scheme can guarantee the QoE level of much more users compared with the conventional scheme. This is why, in case of higher guaranteed QoE level, the conventional scheme accommodates the users that are distant from the adequate distance threshold although it cannot guarantee the QoE level of such users. Additionally, in case of lower guaranteed QoE level, the conventional scheme accommodates only users that are within 70 m although it can accommodate more distant users while satisfying their QoE value. Since a lot of RRHs unnecessarily enter in active state at a time slot and the number of RRHs that can enter in active state will not be enough at the next time slot, the number of users satisfying QoE value in the conventional scheme is lower than that in the proposed scheme. Indeed, the proposed scheme associates much more 55 users while satisfying their QoE value.

Fig. 5(c) shows the cumulative sum of guaranteed users and power efficiency (GUPE) in different QoE environments. Since GUPE denotes how many users can be guaranteed by 1-W

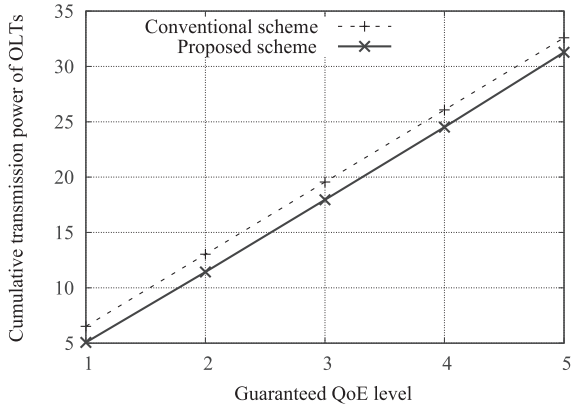

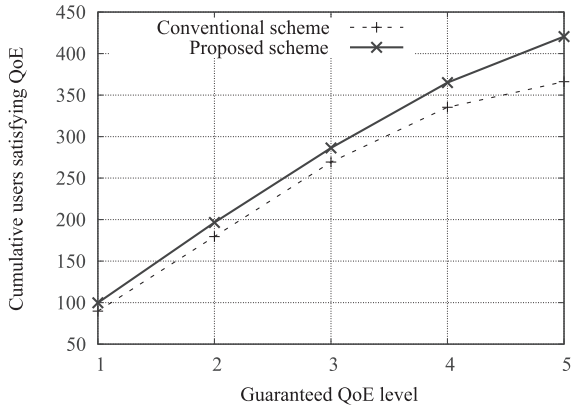

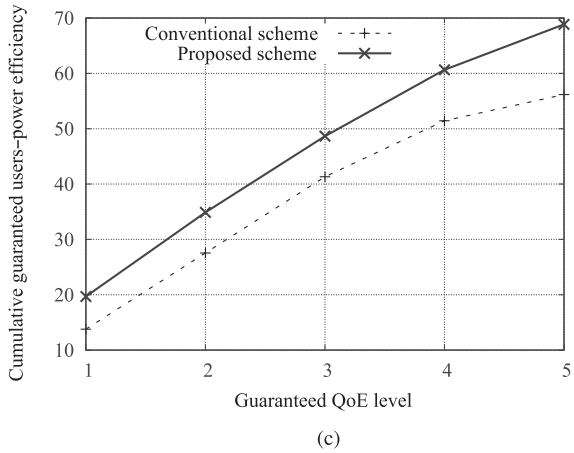

Fig. 5. Performance comparison in different QoE environments.

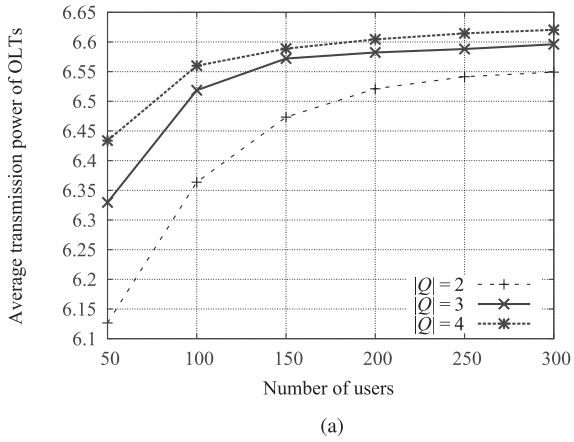

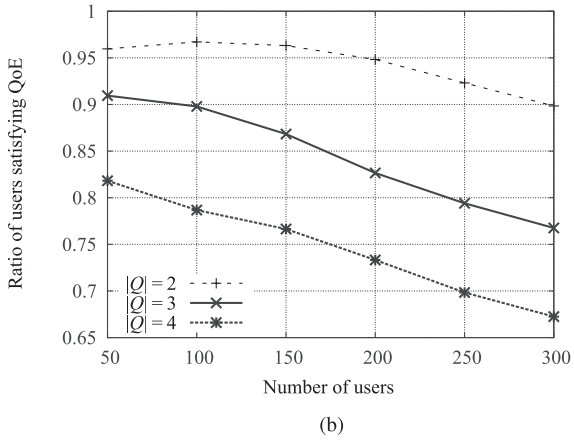

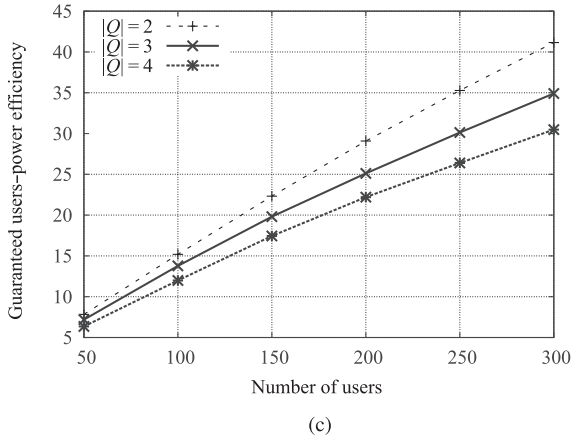

Fig. 6. Performance evaluation in different user densities.

transmission power, the value of GUPE η can be expressed with the number of users satisfying QoE $|U_{\text{guaranteed}}|$, and the average transmission power of OLTs $\langle O \rangle$ as

$$\eta = \frac{|U_{\text{guaranteed}}|}{\langle O \rangle}. \tag{20}$$

From Fig. 5(c), it is clear that our proposed scheme achieves higher GUPE in all QoE settings. The improvement of GUPE rises with increase in the guaranteed QoE level and improvement is 73.7% when the QoE level is 5. This means that the proposed scheme can effectively guarantee QoE level even when users request higher QoE level.

C. Impact of User Density on the Performance of the Proposal

Here, we investigate the performance of our proposed scheme in different user densities. In this simulation, we change the number of users from 50 to 300 in 50 increments. Also, we set three different QoE levels, i.e., $|Q| = 2$, $|Q| = 3$, and $|Q| = 4$, where (19) is used as a QoE function. Additionally, the margin of battery is set to 2 J.

Fig. 6(a) shows the average transmission power of OLTs in different user densities. It is shown that the transmission power logarithmically rises and that there is an upper limitation of transmission power. This phenomenon happens for the following reasons. Since the number of accommodated users

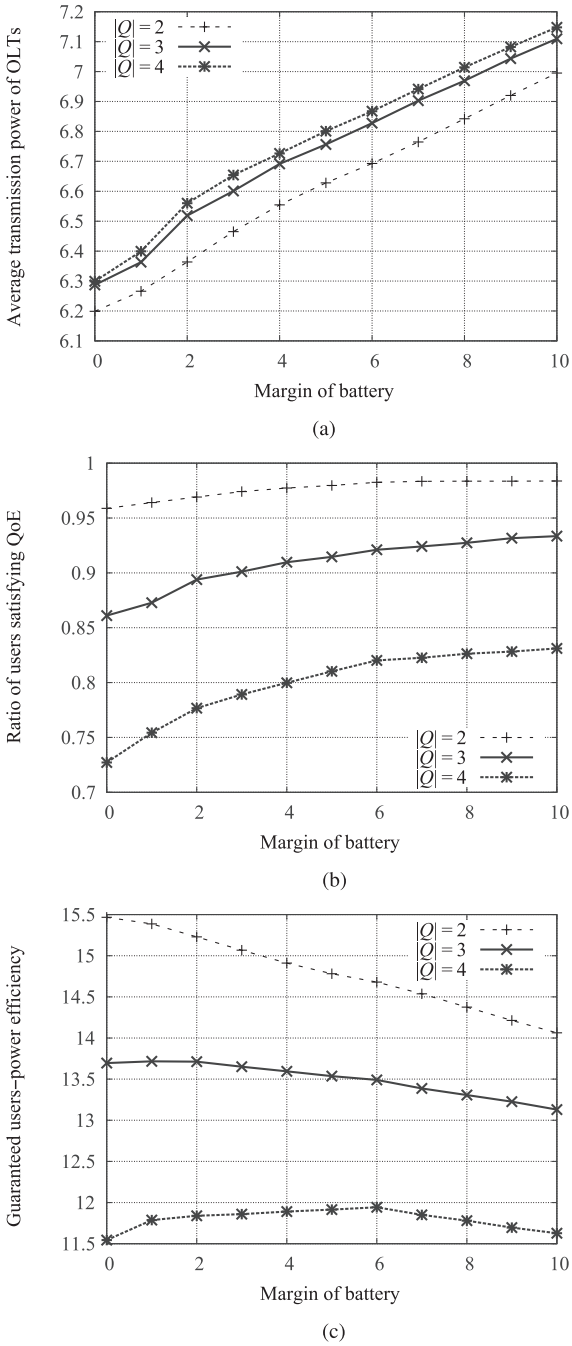

Fig. 7. Performance evaluation when the margin of battery changes.

is limited, the number of RRHs that should enter in active state increases with the increase in user density. Therefore, each OLT needs to increase its transmission power in order to give enough power to the RRHs whose amount of battery is low. On the other hand, since we set a lower bound of battery, which decides whether RRH can enter in active state, the transmission power is limited. Therefore, the transmission power drastically increases when the node density is low and the growth of transmission power is gradual with the increase in user density.

Fig. 6(b) demonstrates the ratio of users satisfying QoE level in different user densities in a setting equal to that of Fig. 6(a). In all cases, the ratio of users satisfying QoE degrades with the increase in user density. This is because, although the number of RRHs in active state should increase to guarantee the QoE level in case of higher user density, some users cannot be accommodated by RRHs since the number of accommodated users and the number of RRHs that can enter in active state at each time slot are limited.

Fig. 6(c) depicts the changes of GUPE in different user densities. As shown in this figure, the increasing rate in low QoE level setting (e.g., $|Q| = 2$) is higher than that in high QoE level setting (e.g., $|Q| = 4$). This indicates that, in case of high user density, the higher we set QoE, the more difficult it is to guarantee QoE level and achieve high power-efficiency.

D. Impact of Margin of Battery on the Performance of the Proposal

This section demonstrates the impact of operation parameter ε, which indicates the margin of battery, on the performance of our proposed scheme. In this simulation, we change the value of ε from 0 to 10 in 1 increment. Additionally, (19) is used as QoE function and the number of users is set to 100.

As shown in Fig. 7(a), the average transmission power of OLTs can be increased by setting a higher margin of battery. This is because this parameter denotes the amount of battery in an RRH that has minimum amount of battery at next time slot and the transmission power of OLTs is decided based on its amount of battery. On the other hand, the ratio of users satisfying QoE level gradually increases with the increase in the margin of battery, as shown in Fig. 7(b). This is caused by the increase of average transmission power. Therefore, the proposed scheme can control the transmission power of OLTs and ratio of guaranteed users by changing the margin of battery. Fig. 7(c) demonstrates GUPE in different margins of battery. From this figure, it is clear that there exists an optimal point for maximizing GUPE and the point depends on the QoE level, e.g., $\varepsilon = 0$ when $|Q| = 2$, $\varepsilon = 1$ when $|Q| = 3$, and $\varepsilon = 6$ when $|Q| = 4$. Consequently, we can conclude that the proposed scheme can effectively guarantee the QoE level by setting the optimal value of ε.

VI. Conclusion

In this paper, we addressed the challenge of QoE-guaranteed and power-efficient network operation for C-RAN based on PON exploiting PoF. To address this challenge, we derived a mathematical model to evaluate the performance of our envisioned C-RAN. Additionally, we constructed a novel framework to evaluate the correlation between the QoE value and transmission distance from RRH to user. This model showed the existence of the distance threshold, in which a certain QoE value of users can be guaranteed. Based on the distance threshold, we proposed an adequate network operation scheme. Our proposed scheme jointly controls the sleep scheduling of RRHs and the transmission power of OLTs to reduce the transmission power while satisfying the QoE value. Extensive simulations demonstrated the effectiveness of our proposed scheme.

REFERENCES

[1] S. Chen and J. Zhao, "The requirements, challenges, and technologies for 5G of terrestrial mobile telecommunication," *IEEE Commun. Mag.*, vol. 52, no. 5, pp. 36–43, May 2014.

[2] E. Dahlman *et al.*, "5G wireless access: Requirements and realization," *IEEE Commun. Mag.*, vol. 52, no. 12, pp. 42–47, Dec. 2014.

[3] M. D. Sanctis *et al.*, "Satellite communications supporting Internet of remote things," *IEEE Internet Things J.*, vol. 3, no. 1, pp. 113–123, Oct. 2015.

[4] J. Wu *et al.*, "Cloud radio access network (C-RAN): A primer," *IEEE Netw.*, vol. 29, no. 1, pp. 35–41, Jan./Feb. 2015.

[5] Z. Zhou *et al.*, "Energy-efficient resource allocation for D2D communications underlaying cloud-RAN based LTE-A networks," *IEEE Internet Things J.*, to be published.

[6] G. Chang, C. Liu, and L. Zhang, "Architecture and applications of a versatile small-cell, multi-service cloud radio access network using radio-over-fiber technologies," in *Proc. IEEE Int. Conf. Commun. (ICC'13)*, Budapest, Hungary, Jun. 2013, pp. 879–883.

[7] M. Gerasimenko *et al.*, "Cooperative radio resource management in heterogeneous cloud radio access networks," *IEEE Access*, vol. 3, pp. 397–406, Apr. 2015.

[8] Y. Guo *et al.*, "Demonstration of a symmetric 40 Gbit/s TWDM-PON over 40 km passive reach using 10 G burst-mode DML and EDC for upstream transmission," *IEEE/OSA J. Opt. Commun. Netw.*, vol. 7, no. 3, pp. A363–A371, Mar. 2015.

[9] N. Shibata *et al.*, "Dynamic IQ data compression using wireless resource allocation for mobile front-haul with TDM-PON," *IEEE/OSA J. Opt. Commun. Netw.*, vol. 7, no. 3, pp. A372–A378, Mar. 2015.

[10] K. Miyanabe *et al.*, "A cloud radio access network with power over fiber toward 5G network: QoE-guaranteed design and operation," *IEEE Wireless Commun.*, vol. 22, no. 4, pp. 58–64, Aug. 2015.

[11] I. Bisio *et al.*, "Gender-driven emotion recognition through speech signals for ambient intelligence applications," *IEEE Trans. Emerging Topics Comput.*, vol. 1, no. 2, pp. 244–257, Jul. 2013.

[12] J. Zhang and N. Ansari, "On assuring end-to-end QoE in next generation networks: Challenges and a possible solution," *IEEE Commun. Mag.*, vol. 49, no. 7, pp. 185–191, Jul. 2011.

[13] M. Dong *et al.*, "Quality-of-experience (QoE) in emerging mobile social networks," *IEICE Trans. Inf. Syst.*, vol. E97-D, no. 10, pp. 2606–2612, Oct. 2014.

[14] M. Dong *et al.*, "QoE-ensured price competition model for emerging mobile networks," *IEEE Wireless Commun.*, vol. 22, no. 4, pp. 50–57, Aug. 2015.

[15] K. Mitra, A. Zaslavsky, and C. Ahlund, "Context-aware QoE modelling, measurement, and prediction in mobile computing systems," *IEEE Trans. Mobile Comput.*, vol. 14, no. 5, pp. 920–936, Dec. 2013.

[16] S. Baraković and L. Skorin-Kapov, "Survey and challenges of QoE management issues in wireless networks," *J. Comput. Netw. Commun.*, vol. 2013, 28 pp., Dec. 2012.

[17] P. Agyapong *et al.*, "Design considerations for a 5G network architecture," *IEEE Commun. Mag.*, vol. 52, no. 11, pp. 65–75, Nov. 2014.

[18] Y. H. Cho *et al.*, "A QoE-aware proportional fair resource allocation for multi-cell OFDMA networks," *IEEE Commun. Lett.*, vol. 19, no. 1, pp. 82–85, Jan. 2015.

[19] K. Saito *et al.*, "A MPCP-based centralized rate control method for mobile stations in FiWi access networks," *IEEE Wireless Commun. Lett.*, vol. 4, no. 2, pp. 205–208, Jan. 2015.

[20] D. Wake *et al.*, "Optically powered remote units for radio-over-fiber systems," *J. Lightw. Technol.*, vol. 26, no. 15, pp. 2484–2491, Aug. 2008.

[21] J. Wei and K. Zhaoyuan, "Design of WDM RoF PON based on OFDM and optical heterodyne," *IEEE/OSA J. Opt. Commun. Netw.*, vol. 5, no. 6, pp. 652–657, Jun. 2013.

[22] H. Nishiyama *et al.*, "A cooperative ONU sleep method for reducing latency and energy consumption of STA in smart-FiWi networks," *IEEE Trans. Parallel Distrib. Syst.*, vol. 26, no. 10, pp. 2621–2629, Oct. 2014.

[23] R. S. Penze *et al.*, "Fiber powered extender for XG-PON/G-PON applications," *IEEE/OSA J. Opt. Commun. Netw.*, vol. 6, no. 3, pp. 250–258, Mar. 2014.

[24] M. Fiedler and T. Hossfeld, and P. Tran-Gia, "A generic quantitative relationship between quality of experience and quality of service," *IEEE Netw.*, vol. 24, no. 2, pp. 36–41, Mar./Apr. 2010.

[25] J. Neckebroek, H. Bruneel, and M. Moeneclaey, "Application layer ARQ for protecting video packets over an indoor MIMO-OFDM link with correlated block fading," *IEEE J. Sel. Areas Commun.*, vol. 28, no. 3, pp. 467–475, Apr. 2010.

[26] T. Hoßfeld *et al.*, "Testing the IQX hypothesis for exponential interdependency between QoS and QoE of voice codecs iLBC and G.711," Univ. Wurzburg, Wurzburg, Germany, Tech. Rep. No. 375, Mar. 2008 [Online]. Available: http://eprints.cs.univie.ac.at/375/

[27] Q. T. Zhang, "Outage probability in cellular mobile radio due to Nakagami signal and interferers with arbitrary parameters," *IEEE Trans. Veh. Technol.*, vol. 45, no. 2, pp. 364–372, May 1996.

[28] M. Xiaomin *et al.*, "MAC and application-level broadcast reliability in vanets with channel fading," in *Proc. Int. Conf. Comput. Netw. Commun. (ICNC)*, San Diego, CA, USA, Jan. 2013, pp. 756–761.

[29] K. Slavakis and G. B. Giannakis, "Online dictionary learning from big data using accelerated stochastic approximation algorithms," in *Proc. Int. Conf. Acoust. Speech Signal Process. (ICASSP)*, Florence, Italy, May 2014, pp. 16–20.

[30] D. Berberidis *et al.*, "Online censoring for large-scale regressions," in *Proc. Asilomar Conf. Signals Syst. Comput.*, Pacific Grove, CA, USA, Nov. 2014, pp. 14–18.

[31] L. Shi and S.-S. Lee, "Energy-efficient PON with sleep-mode ONU: Progress, challenges, and solutions," *IEEE Netw.*, vol. 2012, no. 2, pp. 36–41, Mar./Apr. 2012.

[32] X. Xie *et al.*, "1.8 Watt RF power and 60% power conversion efficiency based on photodiode flip-chip-bonded on diamond," in *Proc. CLEO: QELS-Fundam. Sci.*, 2014, p. JTh5B.9.

Katsuya Suto (S'11) received the M.S. degree in information science from the Graduate School of Information Sciences (GSIS), Tohoku University, Sendai, Japan, in 2013, where he is currently pursuing the Ph.D. degree in information science.

His research interests include big data mining architecture, resilient network design, and wireless networking.

Mr. Suto is a student member of IEICE. He was the recipient of the Prestigious Dean's Award from Tohoku University in March 2013. He was also the recipient of the Best Paper Award at the IEEE 79th Vehicular Technology Conference (VTC'13-spring), the IEICE Academic Encouragement Award in 2014, the IEEE VTS Japan 2015 Young Researcher's Encouragement Award, and the Best Paper Award at the IEEE/CIC International Conference on Communications in China in 2015 (ICCC'15).

Keisuke Miyanabe (S'11) is currently pursuing the M.S. degree in information science at the Graduate School of Information Sciences, Tohoku University, Sendai, Japan.

His research interests include fiber wireless network.

Mr. Miyanabe was the recipient of the IEEE VTS Japan 2014 Student Paper Award.

Hiroki Nishiyama (SM'13) received the M.S. and Ph.D. degrees in information science from Tohoku University, Sendai, Japan, in 2007 and 2008, respectively.

He is an Associate Professor with the Graduate School of Information Sciences (GSIS), Tohoku University. He has authored more than 160 peer-reviewed papers including many high quality publications in prestigious IEEE journals and conference proceedings. His research interests include satellite communications, unmanned aircraft system (UAS) networks, wireless and mobile networks, ad hoc and sensor networks, green networking, and network security.

Dr. Nishiyama is a member of Institute of Electronics, Information, and Communication Engineers (IEICE). He currently serves as an Associate Editor for the IEEE TRANSACTIONS ON VEHICULAR TECHNOLOGY, an Associate Editor for *Springer Journal of Peer-to-Peer Networking and Applications*, and the Secretary of the IEEE ComSoc Sendai Chapter. He was the recipient of Best Paper Awards from many international conference proceedings including IEEE's flagship events, such as the IEEE Global Communications Conference in 2014 (GLOBECOM'14), GLOBECOM'13, GLOBECOM'10, and the IEEE Wireless Communications and Networking Conference in 2014 (WCNC'14), WCNC'12. He was also the recipient of the Special Award

of the 29th Advanced Technology Award for Creativity in 2015, the IEEE Communications Society Asia-Pacific Board Outstanding Young Researcher Award 2013, the IEICE Communications Society Academic Encouragement Award 2011, and the 2009 FUNAI Foundation's Research Incentive Award for Information Technology.

Nei Kato (F'13) received the bachelor's degree in engineering from the Polytechnic University, Tokyo, Japan, in 1986, and the M.S. and Ph.D. degrees in information engineering from Tohoku University, Sendai, Japan, in 1988 and 1991, respectively.

He was an Assistant Professor with the Computer Center, Tohoku University, in 1991, and was promoted to Full Professor with the Graduate School of Information Sciences, in 2003. He became a Strategic Adviser to the President of Tohoku University in 2013, and the Director of Research Organization of Electrical Communication (ROEC), Tohoku University, in 2015. He has authored more than 300 papers in peer-reviewed journals and conference proceedings. His research interests include computer networking; wireless mobile communications; satellite communications; ad hoc, sensor, and mesh networks; smart grid; and pattern recognition.

Dr. Kato serves on the Expert Committee of Telecommunications Council, Ministry of Internal Affairs and Communications, and as the Chairperson of ITU-R SG4 and SG7, Japan. He is a Distinguished Lecturer of the IEEE Communications Society and Vehicular Technology Society. He is a fellow of IEICE. He currently serves as a Member-at-Large on the Board of Governors, the IEEE Communications Society, the Chair of the IEEE Ad Hoc and Sensor Networks Technical Committee, the Chair of the IEEE ComSoc Sendai Chapter, the Editor-in-Chief of the *IEEE Network Magazine*, the Associate Editor-in-Chief of the IEEE INTERNET OF THINGS JOURNAL, and an Area Editor of the IEEE TRANSACTIONS ON VEHICULAR TECHNOLOGY. He has served as the Chair of the IEEE ComSoc Satellite and Space Communications Technical Committee (2010–2012) and the Chair of IEICE Satellite Communications Technical Committee (2011–2012). He was the recipient of the Minoru Ishida Foundation Research Encouragement Prize (2003), Distinguished Contributions to Satellite Communications Award from the IEEE ComSoc, Satellite and Space Communications Technical Committee (2005), the FUNAI Information Science Award (2007), the TELCOM System Technology Award from Foundation for Electrical Communications Diffusion (2008), the IEICE Network System Research Award (2009), the IEICE Satellite Communications Research Award (2011), the KDDI Foundation Excellent Research Award (2012), the IEICE Communications Society Distinguished Service Award (2012), Distinguished Contributions to Disaster-Resilient Networks R&D Award from Ministry of Internal Affairs and Communications, Japan, seven Best Paper Awards from the IEEE GLOBECOM/WCNC/VTC, and the IEICE Communications Society Best Paper Award (2012).

Hirotaka Ujikawa (M'15) received the B.E. and M.E. degrees in computer science from Waseda University, Tokyo, Japan, in 2007 and 2009, respectively.

He is an Engineer with the NTT Access Network Service Systems Laboratories, NTT Corporation, Kanagawa, Japan, since 2009, where he has been engaged in the research and development of optical access systems. His research interests include dynamic bandwidth allocation and dynamic sleep scheduling for energy-efficient access systems.

Ken-Ichi Suzuki (M'08) received the B.E. and M.E. degrees in electronic engineering from Utsunomiya University, Utsunomiya, Japan, in 1988 and 1990, respectively, and the Ph.D. degree in information science and technology from Hokkaido University, Sapporo, Japan, in 2009.

He is a Senior Research Engineer, Supervisor with the NTT Access Network Service Systems Laboratories, NTT Corporation, Kanagawa, Japan, since 1990, where he has been working on research and development of optical communication systems including PON-based optical access systems. His research interests include 10G-EPON systems/technologies and optical amplifier-based long-reach PON systems/technologies.

Dr. Suzuki has been a Vice Chair of the IEEE 1904 Access Network Working Group (former IEEE 1904.1 SIEPON WG). He has been a Director of the Optical Access Test Implementation Liaison Committee in HATS conference of Japan for EPON family interoperability tests. He also serves as a TPC member of OFC2016. He is a member of the Institute of Electronics, the Information and Communication Engineers (IEICE) of Japan, and OPTICAL SOCIETY OF AMERICA (OSA).